Bi-allelic variants in *CEP295* cause Seckel-like syndrome presenting with primary microcephaly, developmental delay, intellectual disability, short stature, craniofacial and digital abnormalities

Niu Li,[a,b,c,d,n] Yufei Xu,[c,n] Hongzhu Chen,[c,n] Jingqi Lin,[b] Lama AlAbdi,[e] Mir Reza Bekheirnia,[f,g,h] Guoqiang Li,[a,b] Yoel Gofin,[f,g] Nasim Bekheirnia,[g,h] Eissa Faqeih,[i] Lina Chen,[c] Guoying Chang,[j] Jie Tang,[c] Ruen Yao,[c,d] Tingting Yu,[c,d] Xiumin Wang,[j] Wei Fu,[k] Qihua Fu,[k,l] Yiping Shen,[c] Fowzan S. Alkuraya,[m] Keren Machol,[f,g,*] and Jian Wang[b,c,d,l,**]

[a]Department of Reproductive Genetics, International Peace Maternity and Child Health Hospital, Shanghai Jiao Tong University School of Medicine, Shanghai, 200030, China
[b]Shanghai Key Laboratory of Embryo Original Diseases, International Peace Maternity and Child Health Hospital, Shanghai Jiao Tong University School of Medicine, Shanghai 200030, China
[c]Department of Medical Genetics and Molecular Diagnostic Laboratory, Shanghai Children's Medical Center, Shanghai Jiao Tong University School of Medicine, Shanghai, 200127, China
[d]Faculty of Medical Laboratory Science, College of Health Science and Technology, Shanghai Jiao Tong University School of Medicine, Shanghai, 200025, China
[e]Department of Zoology, College of Science, King Saud University, Riyadh, 11533, Saudi Arabia
[f]Department of Molecular and Human Genetics, Baylor College of Medicine, Houston, TX, 77030, USA
[g]Texas Children's Hospital, Houston, TX, 77030, USA
[h]Renal Section, Department of Pediatrics, Baylor College of Medicine, Houston, TX, 77030, USA
[i]Department of Pediatric Subspecialties, Children's Hospital, King Fahad Medical City, Riyadh, 11533, Saudi Arabia
[j]Department of Endocrinology and Metabolism, Shanghai Children's Medical Center, Shanghai Jiao Tong University School of Medicine, Shanghai, 200127, China
[k]Institute of Pediatric Translational Medicine, Shanghai Children's Medical Center, Shanghai Jiao Tong University School of Medicine, Shanghai, 200127, China
[l]Shanghai Key Laboratory of Clinical Molecular Diagnostics for Pediatrics, Shanghai, 200127, China
[m]Department of Translational Genomics, Center for Genomic Medicine, King Faisal Specialist Hospital and Research Center, Riyadh, 11211, Saudi Arabia

eBioMedicine
2024;99: 104940
Published Online xxx
https://doi.org/10.1016/j.ebiom.2023.104940

Summary

Background Pathogenic variants in the centrosome protein (CEP) family have been implicated in primary microcephaly, Seckel syndrome, and classical ciliopathies. However, most CEP genes remain unlinked to specific Mendelian genetic diseases in humans. We sought to explore the roles of CEP295 in human pathology.

Methods Whole-exome sequencing was performed to screen for pathogenic variants in patients with severe microcephaly. Patient-derived fibroblasts and CEP295-depleted U2OS and RPE1 cells were used to clarify the underlying pathomechanisms, including centriole/centrosome development, cell cycle and proliferation changes, and ciliogenesis. Complementary experiments using CEP295 mRNA were performed to determine the pathogenicity of the identified missense variant.

Findings Here, we report bi-allelic variants of *CEP295* in four children from two unrelated families, characterized by severe primary microcephaly, short stature, developmental delay, intellectual disability, facial deformities, and abnormalities of fingers and toes, suggesting a Seckel-like syndrome. Mechanistically, depletion of CEP295 resulted in a decrease in the numbers of centrioles and centrosomes and triggered p53-dependent G_1 cell cycle arrest. Moreover, loss of CEP295 causes extensive primary ciliary defects in both patient-derived fibroblasts and RPE1 cells. The results from complementary experiments revealed that the wild-type CEP295, but not the mutant

*Corresponding author. Department of Molecular and Human Genetics, Baylor College of Medicine, Houston, TX, 77030, USA.
**Corresponding author. Central Laboratory, International Peace Maternity and Child Health Hospital, Shanghai Jiao Tong University School of Medicine, Shanghai, 200030, China.
E-mail addresses: Keren.Machol@bcm.edu (K. Machol), Labwangjian@shsmu.edu.cn (J. Wang).
[n]These authors contributed equally.

protein, can correct the developmental defects of the centrosome/centriole and cilia in the patient-derived skin fibroblasts.

Interpretation This study reports *CEP295* as a causative gene of the syndromic microcephaly phenotype in humans. Our study also demonstrates that defects in CEP295 result in primary ciliary defects.

Funding A full list of funding bodies that contributed to this study can be found under "Acknowledgments."

Keywords: Bi-allelic variants of *CEP295*; Centriole and centrosome development; Seckel-like syndrome; Primary microcephaly; Ciliogenesis

Research in context

Evidence before this study

The members of the centrosome protein (CEP) family are active components of the centrosome and therefore play an important role in centriole biogenesis, centrosome assembly, and ciliary biogenesis. Bi-allelic variants of several members of the CEP family have been linked to primary microcephaly (i.e., autosomal recessive primary microcephaly and Seckel syndrome with or without primary microcephaly) and ciliopathies (i.e., Meckel syndrome).

Added value of this study

We revealed *CEP295* as the causative gene related to recessive Seckel-like syndrome. In addition to the confirmation of the centriole and centrosome development defects caused by the *CEP295* mutation in patient-derived fibroblasts, we also showed that ciliary development defects play an important role in the pathogenesis.

Implications of all the available evidence

This study increases our knowledge of the effects of dysfunction of CEPs on human diseases. These findings indicate that *CEP295* variants can lead to the microcephaly phenotype by blocking both centrosome development and ciliogenesis.

Introduction

The centrosome, the primary microtubule-organizing center (MTOC) in eukaryotic cells, is composed of a pair of centrioles (termed mother- and daughter-centrioles) that are surrounded by an electron-dense matrix known as pericentriolar material (PCM). In proliferating cells, the formation of centrioles/centrosomes is strictly regulated by the cell cycle, where the centrioles undergo semi-conservative duplication to ensure cell entry in mitosis, involving two functional centrosomes and a bipolar spindle that arranges chromosomes on the metaphase plate.[1,2] Moreover, the centrosome has a major function in primary ciliogenesis. In non-proliferating cells, the mother centriole migrates to the cell surface to form a basal body, which serves as the template for the formation of cilia.[3] Therefore, structural and/or functional defects in centrosomes/centrioles are closely associated with abnormal cell division and cell cycle progression, chromosomal aneuploidy, and ciliary dysfunction.[1]

The centrosome protein (CEP) family is the active component of the centrosome and is essential for centriole biogenesis. Though hundreds of candidate genes that may encode centrosome-related proteins have been included in the centrosome database (centrosomeDB),[4] as well as in the Cell Atlas (https://www.proteinatlas.org/humanproteome/cell/centrosome), only about 30 related genes have been well characterized and classified as members of the CEP family thus far.[5] CEPs are involved in various developmental stages of the centriole and centrosome. For example, CEP135 plays an important role in centriole elongation,[6] while CEP152 is involved in initiating centriole duplication.[7] Pathogenic variants in CEPs are associated with syndromes that present with microcephaly and neurodevelopmental defects, suggesting that CEPs have a particularly critical role in brain development.[8] Implicated genes include the autosomal recessive primary microcephaly (MCPH)-related genes *CENPJ* (MCPH6, MIM: 608393), *CEP135* (MCPH8, MIM: 614673), *CEP152* (MCPH9, MIM: 614852), and *CEP215* (MCPH3, MIM: 604804) and the microcephalic primordial dwarfism (Seckel syndrome)-related gene *CEP63* (SCKL6, MIM: 614728) (https://omim.org/). Notably, there is a known overlap in the etiology of MCPH and Seckel syndrome, e.g., bi-allelic variants in *CENPJ* and *CEP152* also result in Seckel syndrome (SCKL4, MIM:613676 and SCKL5, MIM: 613823, respectively). In addition, defects in CEPs can lead to classical ciliopathies, such as Joubert syndrome (JBTS) associated with *CEP41* (JBTS 15, MIM: 614464), nephronophthisis (NPHP) associated with *CEP164* (NPHP 15, MIM: 614845), and Meckel syndrome (MKS,

also known as Meckel-Gruber syndrome) associated with *CEP290* (MKS4, MIM: 611134). Most CEP genes, however, remain unlinked to specific Mendelian genetic diseases in humans.

In this study, we identified bi-allelic variants of *CEP295* in four paediatric individuals from two unrelated families showing highly consistent clinical phenotypes, characterized as Seckel-like syndrome with primary microcephaly and short stature. We uncovered defects in centriole biogenesis, centrosome formation, and ciliary biogenesis in patient-derived fibroblasts. Our findings strongly suggest that *CEP295* is a causative gene of Seckel-like syndrome. We further report a foetus with typical features of MKS, including encephalocele and dysplastic kidney, who was assumed to harbour bi-allelic variants of *CEP295* because both the parents were heterozygotes of *CEP295*.

Methods

Patients and ethics

A total of four paediatric patients and one foetus (stillbirth) from three unrelated families were included in this study. Clinical data and DNA specimens were collected and used, following the procedures and protocols in accordance with the ethical standards of the responsible institutional committee on human experimentation and with the Helsinki Declaration of 1975, as revised in 2000. The relevant protocols were approved by the Ethics Committee of Shanghai Children's Medical Center (SCMCIRB-K2020060-1), the Institutional Review Board for Baylor College of Medicine and Affiliated Hospitals (H-29697), and the Ethics Committee of King Faisal Specialist Hospital and Research Centre (KFSHRC RAC#2080006).

Genomic sequencing

For family 1, trio whole-exome sequencing (WES) was performed as previously reported.[9] The parental origin of the *CEP295* variants was confirmed via Sanger sequencing. For family 2, DNA from patients 2 and 3 and their parents was sequenced on a clinical basis using Quad-WES in a CLIA-approved commercial lab (Baylor Genetics). Variants were confirmed in patient 3 following sequencing using the Illumina platform (Baylor Genetics). For family 3, a specimen of the foetus was unavailable, and duo-WES was performed in the parents to screen candidate variants as previously described.[10]

Sanger sequencing for verification of the *CEP295* gene

Primers for amplification of *CEP295* (GenBank accession no. NM_033395.2, https://www.ncbi.nlm.nih.gov/gene/85459) were designed using the Primer 3 online platform (http://primer3.ut.ee/) and are as follows: Exon 13-forward, 5′- CGTGTGTTATCTTTGCCTTTGT-3′; Exon 13-reverse, 5′-TTCTGCATCCTACCCCAGTC-3′; Exon 15-forward, 5′- ACACTTGCATGCACAGACAG-3′; and Exon 15-reverse, 5′- ACGAATGCTCTGTTTCC TTGG -3′. For patient 1 and each of their family members, both exons and exon-intron boundaries were amplified via polymerase chain reaction (PCR; Takara Bio, Dalian, China). The PCR products were examined on a 1% agarose gel, purified using a QIAquick Gel Extraction Kit (Qiagen GMBH, Hilden, Germany) according to manufacturer's instructions, and sequenced using an ABI3730XL sequencer (Applied Biosystems, Foster City, CA, USA).

Skin fibroblast isolation and cell culture

After informed consent was obtained, skin fibroblasts were derived from the patient of family 1 and two sex- and age-matched healthy control individuals. U2OS (RRID:CVCL_0042) and hTERT-immortalized RPE1 (RRID:CVCL_4388) cells were maintained in Dulbecco's modified Eagle's medium (DMEM, Hyclon) supplemented with 10% foetal bovine serum (GIBCO) and 1% penicillin/streptomycin (GIBCO) at 37 °C in a humidified 5% CO_2 incubator. 2 mM of L-glutamine (GIBCO) was added to the human fibroblast culture.

siRNA transfection

siRNA oligonucleotides were transfected into cells using Lipofectamine RNAiMAX Reagent (Life Technologies) according to the manufacturer's instructions. The sequences of the siRNAs used in this study were as follows: negative control (siCtrl), GGGUAUCGACGAUUA CAAA; siCEP295, GCAUGAACUUAGUGCUAUA.

mRNA synthesis and transfection

mRNA was synthesized as previously described.[11] Briefly, the WT and c.1685C > T mutant CEP295 mRNA integrated with Myc tag at the C-terminal were produced using T7 RNA polymerase-mediated transcription, respectively, from a linearized DNA template incorporating generic 5′and 3′ UTRs and a poly(A) tail. To enhance the *in vitro* stability and protein translation, uridine was replaced with N1-methylpseudouridine during the synthesis procedure. The mRNA was purified using an Ambion MEGAclear kit (Thermo Fisher Scientific) and treated with Antarctic Phosphatase (New England Biolabs, Ipswich, MA, USA) for 30 min at 37 °C to remove residual 5′-phosphates. The mRNA resuspended in 10 mM Tris HCl with 1 mM EDTA was transfected into patient 1-derived fibroblasts with the dose of 2 μg/250,000 cells using the ExPERT ATx™ electroporation systems according to the manufacturer's instructions (MaxCyte Rockville, MD, USA).

Western blot and antibodies

Cells were lysed with sodium dodecyl sulfate lysis buffer (100 mM Tris–HCl [pH 6.8], 10% glycerol, and 1% SDS). The lysates containing equal amounts of protein were subjected to 10% bis-tris gel (ThermoFisher

Scientific) electrophoresis and transferred onto polyvinylidene fluoride membranes. The membranes were blocked using 5% non-fat milk in TBS-T for 1 h and then incubated overnight at 4 °C with the following antibodies: anti-p53 (Cell Signaling Technology #2527, RRID:AB_10695803), anti-p21 (Cell Signaling Technology #2947, RRID:AB_823586), and anti-actin (Cell Signaling Technology #4967, RRID:AB_330288). To detect endogenous human CEP295, we generated rabbit polyclonal antibodies against CEP295 (residues 1–163).

Immunofluorescence

To determine the numbers of centrosomes in the S-phase, fibroblasts cultured on coverslips in a 12-well plate were double blocked with 2 mM thymidine (arrested for 16 h, released for 8 h, and arrested for another 16 h), and then the cells were released for another 5 h. Then, the cells were washed with 1 x PBS and fixed using 4% paraformaldehyde at room temperature for 15 min. The coverslips were then washed with 1 x PBS three times and blocked (blocking buffer, 1x PBS/5% goat serum/0.3% Triton X-100) for 1 h. The samples were co-incubated with anti-centrin (Sigma–Aldrich # 04-1624) and anti-γ-tubulin (GeneTex # GTX113286, RRID:AB_1952442) or anti-PLK4 (Proteintech, #12952-1-AP, RRID:AB_2284150) and anti-SAS-6 (Proteintech, #21377-1-AP, RRID:AB_2878851) overnight at 4 °C. The samples were then labelled with goat anti-rabbit IgG (H + L) secondary antibody (Life Technologies #A32731) and goat anti-mouse IgG (H + L) secondary antibody (Life Technologies # A32727).

To examine ciliary development in the absence of CEP295, fibroblasts or RPE1 cells transfected with control or CEP295 siRNA for 24 h were starved for another 24 h on coverslips in a 12-well plate. After fixation and blocking, the samples were co-stained with anti-ARL13B (Proteintech, #17711-1-AP, RRID:AB_2060867) and anti-centrin (Sigma–Aldrich, #04-1624).

To determine the rescue efficiency of the development of centrosomes and centrioles, 24 h after transfection with CEP295 mRNA, the fibroblasts were then synchronized at S-phase by thymidine and were co-stained with anti-Myc-tag (Cell Signaling Technology, Cat# 2276; RRID:AB_3317) and anti-γ-tubulin or anti-PLK4. To observe the rescue efficiency of ciliary formation, the fibroblasts were transfected with CEP295 mRNA for 48 h and were starved for another 24 h after on coverslips. Cells were then co-stained with anti-Myc and anti-ARL13B. The samples were then labelled with the above-indicated secondary antibodies and observed using a Leica DM6000B fluorescence microscope.

Cell proliferation assay

U2OS cells were transfected with control or CEP295 siRNAs in a 6-well plate. After 6 h, the cells were seeded in a 96-well plate (1000 cells/well). The cell viability for 6 days was determined using the Cell Counting Kit-8 (CCK-8) assay kit (Dojindo, Kumamoto, Japan), and the cell growth curve was plotted.

Cell cycle analysis

After 48 h of transfection with control (Ctrl) or CEP295 siRNAs, U2OS cells were collected after digestion with trypsin and were washed twice with 1 × cold-PBS. The cells were then fixed in 70% ethanol at –20 °C overnight and stained with FxCycle™ PI/Rnase staining solution (Thermo Fisher Scientific #F10797) for 20 min. Cell cycle distribution was analysed using a FACS Canto™ flow cytometry system (BD Biosciences). The data were analysed using Modfit LT software v5.0 (Verity Software House).

Quantitative RT-PCR

Total RNA was extracted from human fibroblasts using an Rneasy Mini kit (Qiagen) according to the manufacturer's instructions, and cDNA was obtained using an RT kit (TaKaRa). Quantification of gene expression was performed in triplicate using Bio-rad iQ SYBR Green Supermix (Bio-Rad) and was detected on the Realplex system (Eppendorf). The following primers were used for qPCR: *GLI1*: forward, 5′-ACATCAACTCCGGCCAATAG-3'; reverse, 5′- GAGGATGC TCCATTCTCTGG -3'; *PTCH1*: forward, 5′- ACCTGC TCTCCCAGTTCTCC -3'; reverse, 5′- ATTCTCTGG TTTCCCGAGGT -3'; *GAPDH* (Human): forward, 5′-CCATCTTCCAGGAGCGAGAT-3'; reverse, 5′- TGCTG ATGATCTTGAGGCTG-3'.

Reverse transcription polymerase chain reaction (RT-PCR)

Wild-type mice of C57BL/6 background were purchased from Shanghai Model Organisms Center, Inc. and housed in standard cages in a pathogen-free facility. To determine the expression pattern of *Cep295* in mouse brain, four pregnant mice at different embryonic stages (E10.5, E11.5, E13.5, and E14.5) were euthanized using carbon dioxide. Total RNA was then extracted from the whole brains of the foetal mice using Trizol (Roche) according to the manufacturer's instructions, and cDNA was obtained using an RT kit (TaKaRa). The leader of the project was aware of the group allocation at the different stages of each experiment. All animal experiments complied with the ARRIVE guidelines and were conducted according to protocols approved by the Institutional Animal Care Committee of Shanghai Children's Medical Center.

The following primers were used for PCR amplification of a 337-bp fragment of *Cep295* (NM_176976.5) cDNA: forward (located on exon 2), 5′-TGAGCCC-TAGTGAAGAAGCC-3′; reverse (located on exon 4), 5′-TGCCTCACTTCTGCTTTTCT-3′. A 245-bp region of *Gapdh* was used as an internal control, and the following primers were used for amplification:

forward, 5′-TGTTTGTGATGGGTGTGAACC-3′; reverse, 5′-AGTGGATGCAGGGATGATGT-3′.

Statistical analysis

All quantitative data were analyzed using GraphPad Prism 8 software. All values are represented as mean ± SEM (or SD where appropriate) as indicated in figure legends. The statistical significance of differences was assessed using the Student's t-test for the comparison of two groups and one-way analysis of variance (ANOVA) with Tukey's test for the comparison of multiple groups. *P*-values less than 0.05 were considered statistically significant.

Role of funders

The funding sources were not involved in the study design, the analysis and interpretation of the data, the writing of this manuscript, or in the decision to submit this manuscript for publication.

Results

Identification of bi-allelic *CEP295* variants

A Chinese descent male proband (patient 1 in family 1) with physically healthy and non-consanguineous parents (Fig. 1a) was referred to Shanghai Children's Medical Center to seek the underlying genetic cause of microcephaly and growth retardation. A series of candidate genes, including *CABP1*, *CEP295*, *FANCM*, *GLI3*, *KMT2C*, *NCAPD3*, *PCLO*, and *PTRH1*, were identified through WES (Table S1). After prioritization, the compound heterozygous nonsense variants of c.1630C > T, p(Q544*) and c.4558C > T, p(R1520*) in the *CEP295* gene (NM_033395.2) were identified as the top candidates, which were confirmed via Sanger sequencing (Figure S1a). Since *CEP295* was not associated with any human genetic disorders, we tried to identify more patients. Using GeneMatcher,[12] we identified three patients (an elder sister and a pair of identical male twins), from a non-consanguineous family of Hispanic descent (family 2), harbouring a compound heterozygous frameshift variant c.163_164 del, p(R55Efs*49) and a missense variant c.1685C > T, p(P562L) of *CEP295* (Fig. 1a and Figure S1b).

Among the mentioned *CEP295* variants, p.Q544* was absent in the control population databases (gnomAD and ExAC). The other three variants had extremely low allele frequency (Table S2), and no homozygous individuals were listed in the gnomAD database for any of the variants. Additionally, all four variants were absent from our internal repository, composed of approximately 12,000 exomes data. The missense variant c.1685C > T, p.P562L is predicted to be deleterious, according to SIFT ("Damaging," score = 0.001), PolyPhen-2 ("Possibly damaging," score = 0.923), PROVEAN ("Damaging," score = –4.53), CADD ("Damaging," score = 23.5), and ReVe ("Pathogenic," score = 0.88).

Human *CEP295* maps to chromosome 11q21 and comprises 30 exons, encoding a large centrosomal protein (2601 amino acid), which is composed of an N-terminal DDC8-like domain present in the C-terminal of the Ana-1 (PICA) motif and an Alstrom syndrome (ALMS)-like motif at the C-terminal.[13] The four variants are distributed in exons 3, 13, 14, and 15. Of them, the nonsense and two frameshift variants are furthest from the C-terminal (Fig. 1b) and thus likely to cause nonsense-mediated decay. *CEP295* is widely expressed in various human tissues, with the highest expression in the human cerebellum, cerebral cortex, and tibial nerve, according to the human RNA-seq data presented in the Genotype-Tissue Expression (GTEx, https://gtexportal.org) project (Figure S2a). Our RT-PCR data from mouse brain tissues showed that *cep295* was expressed from the early stage of embryonic development (Figure S2b). In addition, analysis of the single-cell transcriptome data of the human cortex from the Allen Brain MAP database (https://celltypes.brain-map.org) showed that *CEP295* is moderately expressed in various types of neurons, including cortical plate-derived excitatory neurons and ganglionic eminence-derived inhibitory neurons (Figure S3). These findings indicate that CEP295 is involved in multiple processes of neural development and further suggest that bi-allelic *CEP295* variants could contribute to neurological defects.

Phenotypic description of the affected patients

The affected individuals included four paediatric patients (three male and one female patient(s)), with ages ranging from 3-month to 9-year-9-month at last clinical evaluation (Fig. 1c, and Table 1). Common features of the patients in families 1 and 2 included severe microcephaly, global developmental delay (GDD), mild intellectual disability (ID), short stature, pachygyria and simplified gyri, and facial dysmorphism including arched eyebrows, prominent nasal bridge, prominent ears, long and smooth philtrum, thin upper lip, and micrognathia. In addition, malformations of fingers and toes were observed, including clinodactyly of the right thumb and syndactyly between the 1st and 2nd fingers of the right hand in patient 1 and 2nd and 5th finger clinodactyly and broad 2nd toe in the patients of family 2 (Fig. 1c). Moreover, abnormalities of the eyes, heart and urinary system were reported in the indicated patients (Table 1). Notably, patient 1 exhibited a gradual slowing of the rate of growth. He had a height of 119.2 cm (–1.94 SD) at 8 years of age, while his height was 125 cm (–2.4 SD) at 9.5 years and was thus, diagnosed with short stature according to the height standard for Chinese children.[14] X-ray imaging showed that his bone age was equivalent to that of a 7-year-old child (Fig. 1c). He had normal levels of growth hormone.

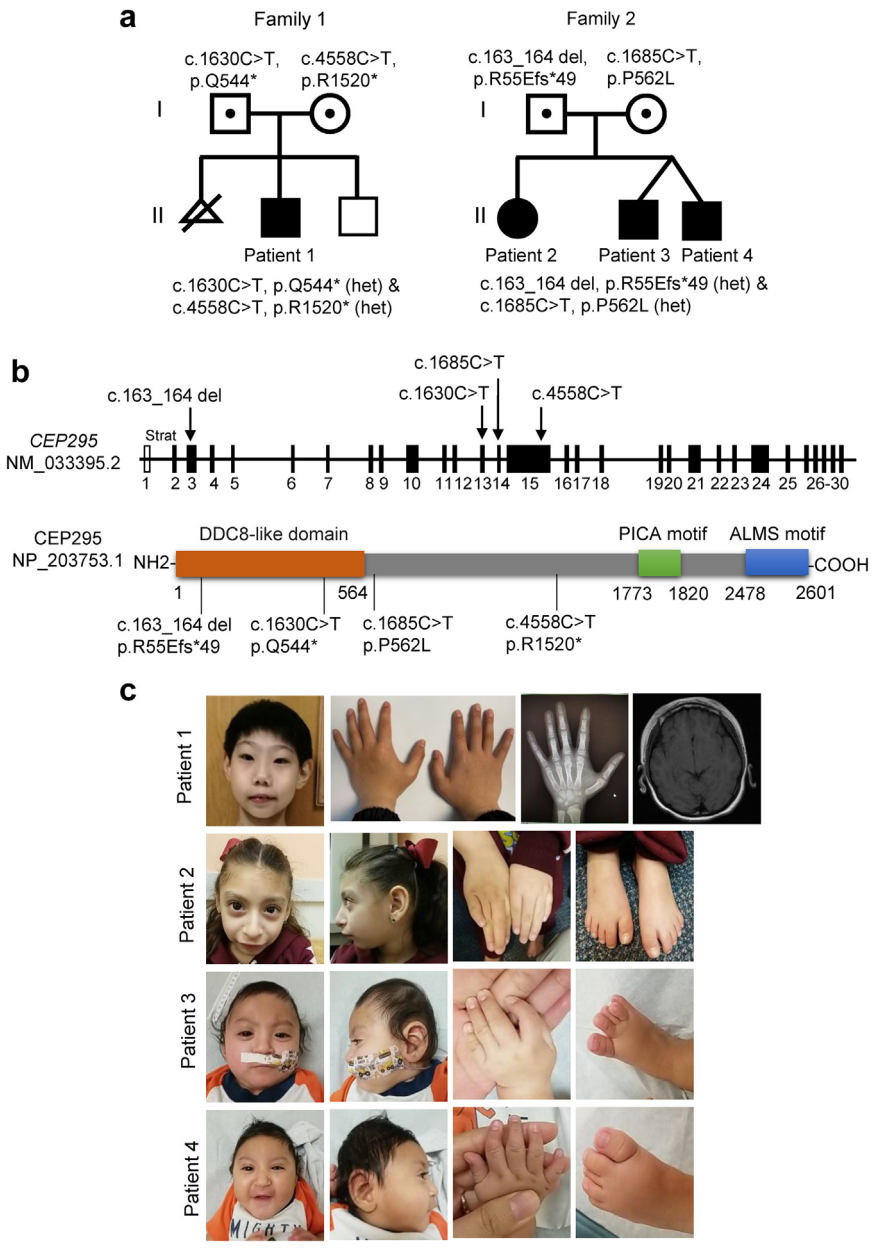

Fig. 1: **Identification of *CEP295* variants in patients with syndromic microcephaly. (a)** A diagram showing two pedigrees in this study. Het, heterozygous; hom, homozygous. **(b)** Top panel, schematic representation of the genomic structure of human *CEP295*. A total of 30 exons are shown as bars, and solid bars represent coding exons. Below them, the protein structure of CEP295 is shown with a DDC8-like (differential display clone 8) domain at its N-terminus, PICA (present in C-terminal of Ana-1) motif, and ALMS (Alstrom syndrome) motif at the C-terminus. The position of each variant is marked by arrows. **(c)** Clinical features of the patients. Patients 1–4 from families 1 and 2 presenting with microcephaly and similar facial dysmorphism, including arched eyebrows, abnormal palpebral fissures, prominent nasal bridge, long or (and) smooth philtrum, prominent ears, micrognathia, and thin upper lip. Patient 1 had syndactyly of the right thumb and underwent surgical treatment at 6 months old. He also had delayed bone age (equivalent to seven years old) and pachygyria. Clinodactyly (2nd and 5th) and broad toe (2nd) were observed in the patients from family 2.

Patient	1 (Family 1)	2 (Family 2)	3 (Family 2)	4 (Family 2)
Sex	Male	Female	Male	Male
Age	9-year-9-month	4-year-7-month	3-month	3-month
Origin	China	Latin-American	Latin-American	Latin-American
Height (cm)	125 (−2.4 SD)	101.6 (−1.13 SD)	46 (−4.3 SD[a])	49.5 (−3.1 SD)
Weight (kg)	28 (−0.9 SD)	15.6 (−0.77 SD)	2.64 (−4.44)	2.74 (−4.24 SD)
HC (cm)	45 (<<−3SD)	42.1 (−5.2 SD)	29 (−6.57 SD)	30.5 (−5.5 SD)
Bone age	7-year	ND	ND	ND
Birth history	C-section at 41 weeks GA	IUGR, C-section at 36 weeks GA.	IUGR, C-section at 30 weeks GA	
Birth length (cm)	48 (−1.0 SD)	41 (−2.52 SD)	35.6 (−1.68 SD)	34.9 (−2.08 SD)
Birth weight (kg)	3.45 (0.3 SD),	1.5 (−2.93 SD)	0.78 (−1.44 SD)	0.88 (−1.59 SD)
Birth HC (cm)	31.5 (−2.3 SD)	27.5 (−3.47 SD)	23 (−3.13 SD)	22 (−3.83 SD)
Craniofacial features				
Microcephaly	+	+	+	+
Arched eyebrows	+	+	+	+
Prominent nasal bridge	+	+	+	+
Prominent ears	+	+	+	+
Long and smooth philtrum	+	+	+	+
Thin upper lip	+	+	+	+
Micrognathia	+	+	–	–
Retrognathia	–	+	–	+
Hanging columella	–	+	–	+
Long tubular nose	–	+	+	+
Slopping forehead	–	–	+	+
Others	Up-slanting palpebral fissures, absence of cupid bow, widely spaced teeth	Down-slanting palpebral fissure, high arched palate, crowded teeth		
Skeletal abnormalities				
Clinodactyly	Right thumb	5th fingers of both hands	2nd and 5th fingers of both hands	2nd and 5th fingers of both hands
Broad 2nd toe	–	Both feet	Both feet	Both feet
others	Syndactyly of the right hand (the 1st and 2nd fingers), surgery was performed at 1 year old			
Developmental and neurology				
Motor delay	+	+	ND	ND
Speech delay	+	+	ND	ND
Intellectual disability	Mild	Mild	ND	ND
Teething delay	Yes, at 1.5-year old	ND	ND	ND
Brain MRI	Pachygyria and simplified gyral pattern	ND	Simplified gyral pattern	Pachygyria and simplified gyral pattern
Echocardiogram	–	Stretched PFO and small secundum ASD, mild left pulmonary artery stenosis	PDA (resolved)	Small PDA (resolved) Small ASD (resolved)
Feeding difficulties	–	+	+ (G-button)	+ (NG-Tube)
Others				
	Myopia of both eyes, strabismus		Tracheoesophageal fistula, left mild hydronephrosis, undescended left testis	
Molecular information				
Variant (CEP295: NM_033395.2)	c.1630C > T,p.Q544* (het)/ c.4558C > T,p.R1520*(het)	c.163_164del p.R55Efs*49(het)/c.1685C > T, p.P562L (het)		

Abbreviations: ASD, atrial septal defect; C-section, cesarean section; GA, gestational age; het, heterozygous; HC, head circumference; hom, homozygous; IUFD, intrauterine fetal death; IUGR, intrauterine growth restriction; MRI, magnetic resonance imaging; ND, not determined because of non-availability or non-applicability; PDA, patent ductus arteriosus; PFO, patent foramen ovale; SD, standard deviation. [a]For patients 3 and 4, Fenton growth curves for premature infants were used.

Table 1: **Clinical features of affected individuals harboring *CEP295* variants.**

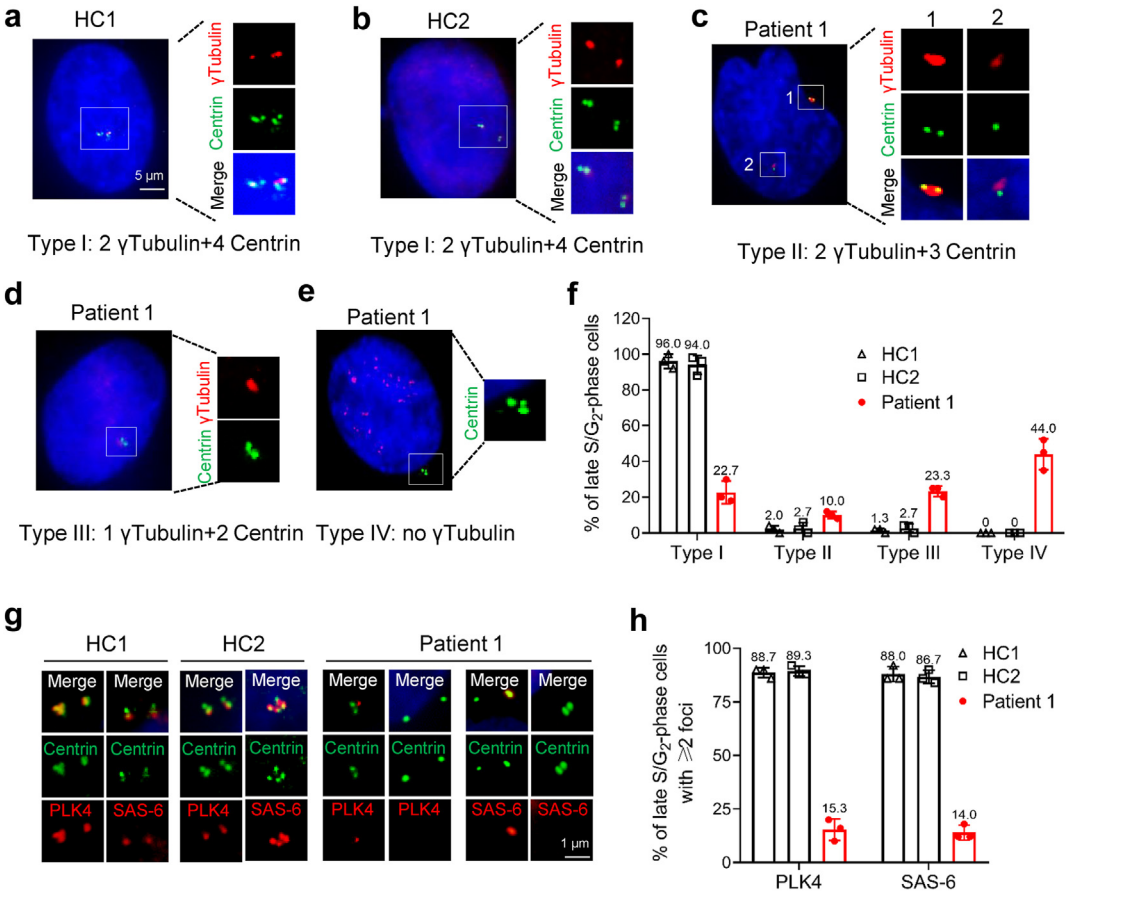

Fig. 2: **Patient-derived fibroblasts show defective CEP295 expression and aberrant centrosome development. (a–e)** The control- and patient-1-derived fibroblasts were blocked at the late S/G_2 phase. Cells were then co-incubated with anti-centrin (green, indicating centriole) and anti-γ-tubulin (red, indicating centrosome). Representative images showing normal centriole-centrosome development (Type I) and three types of centriole-centrosome development defects (Type II-IV). **(f)** Quantification analysis of the centriole-centrosome development defects as indicated in a-e. One hundred cells were analysed for each group from three independent experiments. Data are shown as mean ± SD compiled from three independent experiments **(g, h)** Representative images and quantification analysis to show the recruitment levels of PLK4 and SAS-6 to centrioles in control- and patient-derived fibroblasts, respectively. One hundred cells were analysed from each group. Data are shown as mean ± SD compiled from three independent experiments.

Patient-derived fibroblasts exhibit developmental defects of centrioles and centrosomes

CEP295 was recently identified as a key regulator of daughter-to-mother centriole conversion and centriole-to-centrosome conversion. Depletion of CEP295 in U2OS and HeLa cells results in centrosome reduction and abnormal numbers of centrioles.[13,15] We hypothesized that such defects were also found in patient-derived cells. We derived skin fibroblasts from patient 1 and two healthy controls (HC1 and HC2), and the cells were then synchronized to S/G_2-phase using thymidine to examine the numbers of centrioles and centrosomes. In control fibroblasts, almost all cells showed the expected development of centrioles (labelled with anti-centrin) and centrosomes (labelled with anti-γ-tubulin), displaying two doublets (Type I, two centrosomes and four centrioles), while the proportion of this type of cells in the patient's fibroblasts was only about 20%. Instead, cells with reduced numbers of centrioles and/or centrosomes (Type II-IV) were largely increased in patient 1 (Fig. 2a–f). Interestingly, nearly half of the patient's fibroblasts displayed *de novo* centrioles without centrosome formation (Type IV) (Fig. 2e and f), a pattern only seen in 5% of CEP295-knockdown U2OS cells.[15]

It has been reported that depletion of CEP295 in HeLa cells affected the centriolar recruitment of critical factors, such as PLK4 and SAS-6, to new mother centrioles in interphase cells.[13] We hypothesized that this may also happen in patient-derived fibroblasts. As expected, most of the control fibroblasts showed normal recruitment of PLK4 and SAS-6 to the new mother centrioles in S/G_2-phase cells. However, patient 1's

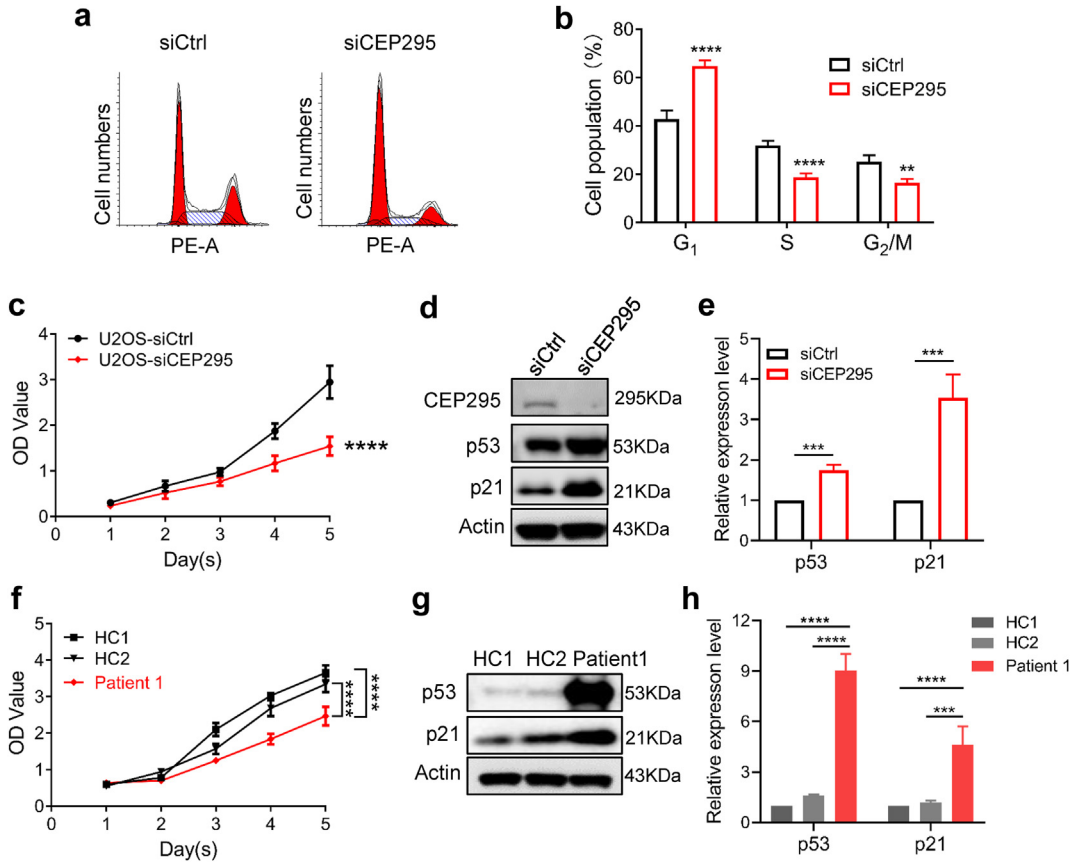

***Fig. 3:* Depletion of CEP295 results in cell growth inhibition and cell cycle arrest via activation of p53-p21 signalling. (a and b)** The cell cycle was analysed in U2OS cells after 48 h of transfection with indicated siRNA. Data are shown as mean ± SD compiled from three independent experiments. ns, no significance; **, $P < 0.01$; ****, $P < 0.0001$; two-tailed Student's t-test. **(c)** Cell viability was determined using CCK-8 cell proliferation assays every 24 h after transfection of the indicated siRNA in U2OS cells. Data are shown as mean ± SD compiled from three independent experiments. ****, $P < 0.0001$; two-way ANOVA test. **(d)** U2OS cells were transfected with indicated siRNA, the cells were lysed after 48 h, and Western blot analyses were performed to determine the expression levels of p53 and p21. **(e)** p53 and p21 levels in CEP295-depleted U2OS cells presented in (d) were normalized to actin levels and then compared with those of the siCtrl group. Data presented are mean ± SD from three independent experiments. ns, not significant; ***, $P < 0.001$; two-tailed Student's t-test. **(f)** Cell viability was determined using CCK-8 cell proliferation assays every 24 h in fibroblasts derived from patient 1 and two healthy controls. Data are shown as mean ± SD compiled from three independent experiments. ****, $P < 0.0001$; two-way ANOVA test **(g and h)** Western blot and statistical analyses to determine the expression levels of p53 and p21 in the fibroblasts. Data are shown as mean ± SD compiled from three independent experiments. ***, $P < 0.001$; ****, $P < 0.0001$.

fibroblasts had obvious defects in centriolar loading of the two critical factors (Fig. 2g and h). These results are indicative of defects in the centriole and centrosome development in patient 1's cells harbouring bi-allelic truncating variants of *CEP295*.

Loss of CEP295 causes p53-dependent cell cycle arrest at the G_1 phase

Given that CEP295 is required for centrosome development, and since centrosomes have a central role in regulating cell cycle progression,[1] we expected that CEP295 defects would affect the cell cycle. To test this hypothesis, we knocked down *CEP295* expression in U2OS cells using siRNA. Flow cytometry analysis at 48 h after transfection indicated that depletion of CEP295 resulted in cell cycle arrest at the G_1 phase (Fig. 3a and b). Consistent with changes in the cell cycle, the depletion of CEP295 caused significant proliferation inhibition, which was reflected in the growth curve results (Fig. 3c). In addition, the expression levels of p53 and its downstream component p21 were significantly elevated in CEP295-depleted U2OS cells (Fig. 3d and e), which is in line with previous observations that centrosome loss after inhibition of PLK4 induces p53 and p21 activation and causes G1-phase arrest.[16–18] Consistently, we showed that the patient-derived fibroblasts also inhibited proliferation and abnormal activation of the p53-p21 signal (Fig. 3f–h). Together, these

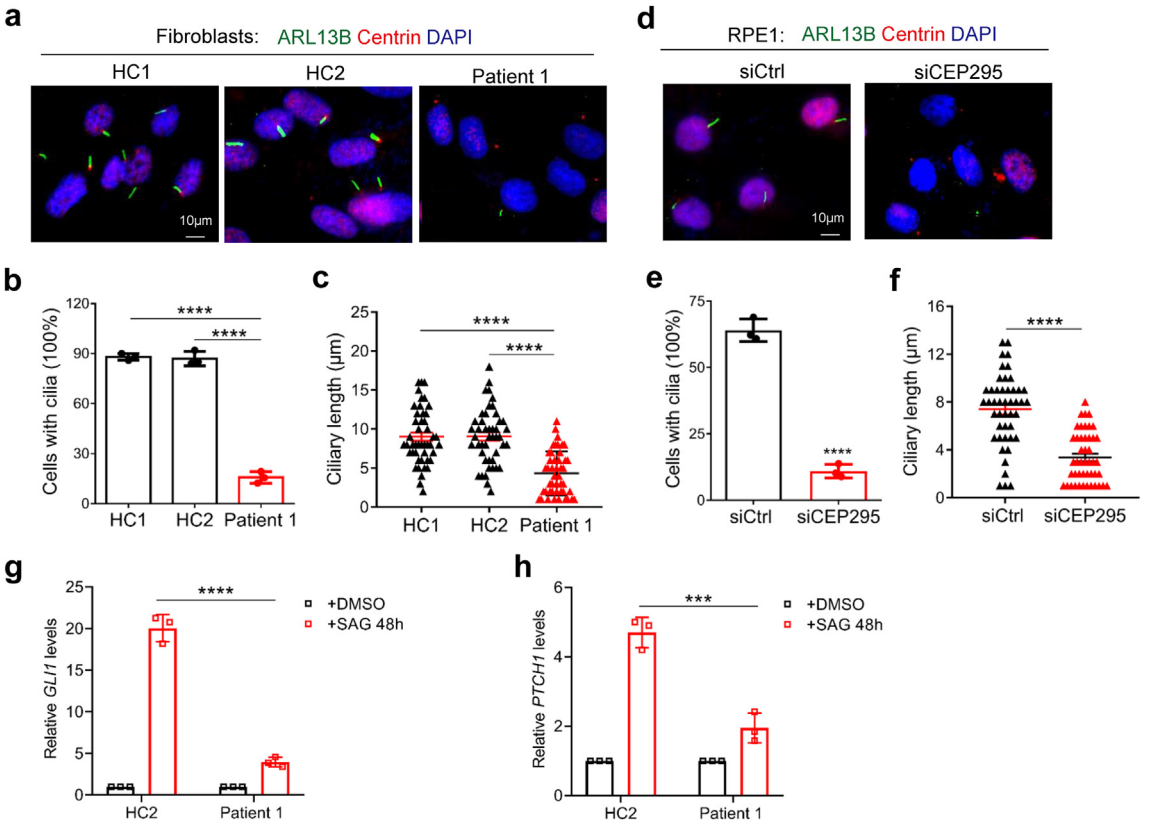

Fig. 4: **Depletion of CEP295 results in ciliary defects. (a)** Representative images of control and patient's fibroblasts stained for centrin (red, indicating centriole) and co-stained for ARL13B (green) to indicate cilium. Cells were treated with serum starvation for 24 h before fixation. **(b)** Quantification of cells with cilia from healthy controls and a patient with CEP295 mutant. More than 150 cells from three independent experiments were quantified for each group. ****, $P < 0.0001$, two-tailed Student's t-test. **(c)** Quantification of the ciliary length of the fibroblasts. A total of 50 ARL13B-positive cells from three independent experiments were quantified for each group. ****, $P < 0.0001$, two-tailed Student's t-test. **(d)** Representative images of RPE1 cells co-stained for centrin and ARL13B after transfection with the indicated siRNA for 48 h **(e, f)** Quantification of cells with cilia (>150 cells) and ciliary length (50 cells) in RPE1 cells after knockdown of CEP295. ****, $P < 0.0001$, two-tailed Student's t-test **(g, h)** Fibroblasts from control 2 and patient 1 were subjected to serum starvation for 24 h. After treatment with SAG (100 nM) or DMSO for an additional 48 h, the expression of *GLI1* and *PTCH1* were determined via qRT-PCR. Data are shown as mean ± SD compiled from three independent experiments. ***, $P < 0.001$; ****, $P < 0.0001$; two-tailed Student's t-test.

results indicated that loss of CEP295 triggers G_1-phase arrest in a p53-dependent manner.

CEP295 is required for ciliary biogenesis in humans

Given that CEPs are required for ciliogenesis, and variants in several of them are known to cause ciliopathies, such as MKS and JBTS,[19–21] we subsequently investigated whether CEP295 is involved in ciliary formation. We examined ciliary formation by staining ARL13B in the control and patient's fibroblasts. On average, nearly 85% of control cells had clear primary ciliary formation after 24 h of serum starvation. In contrast, the patient's fibroblasts had a 3-fold reduction in ciliary formation (Fig. 4a and b). In addition, the cilia of the patient cells were much shorter than those of the control cells (Fig. 4c). Similar results were observed in the RPE1 cells after the knockdown of CEP295 using specific siRNA (Fig. 4d–f). It is well known that the primary cilium is required for the vast majority of signalling pathways, especially for Hedgehog signalling.[22,23] We, therefore, examined if loss of CEP295 affects Hedgehog signalling in the patient fibroblasts. After serum starvation and treatment with smoothened agonist (SAG), control fibroblasts showed significant upregulated of *GLI1* and *PTCH1* mRNA expression, suggesting activation of the Hedgehog signalling pathway. In contrast, the response of the patient's cells was largely attenuated (Fig. 4g and h). Our results strongly suggest that CEP295 is essential for ciliary formation and signalling in human cells.

Intriguingly, a stillbirth male foetus with encephalocele and dysplastic kidney and a clinical diagnosis of MKS was presumed to harbour the homozygous frameshift variant c.2603delA, p.(Q868Rfs*25) in *CEP295*, as duo-WES analysis revealed that both parents

carried the heterozygous variant[10] (Figure S4). Though we were unable to assess clinical features in detail, several clinical features, including a triangle face, depressed nasal bridge, broad mouth, mild retrognathia, and brachydactyly, were observed in available photographs suggesting that the foetus had a syndromic disease. These observations suggest that the variants of *CEP295* may be related to ciliopathy phenotypes and further support the important role of CEP295 in ciliogenesis.

The P562L variant failed to restore centrosome/centriole and ciliary defects in patient-derived fibroblasts

To confirm the pathology of CEP295 and also to determine the pathogenicity of the c.1685C > T (p.P562L) variant identified in family 2, we next attempted to replenish CEP295 in patient 1-derived fibroblasts and observe the development of centrosome/centriole and cilium. The length of *CEP295* cDNA poses a huge challenge for lentivirus construction, making it difficult to stable express CEP295 in human cells. We therefore tried expression of exogenous CEP295 using electroporation with *in vitro* synthesized mRNAs, which has been proven to efficiently achieve exogenous protein expression in various types of mammalian cells.[11,24] Approximately 85% of the WT-CEP295 (Myc)-positive fibroblasts showed clear centrosome structures (Fig. 5a and b), which is quite close to the proportion in the healthy control individuals (Fig. 2a and b). In contrast, only ~10% of the mutant CEP295-positive cells could observe centrosome formation. In addition, replenishment of the WT-CEP295, rather than the P562L mutant, can largely restore the defects of PLK4 recruitment, indicating that the centrioles replication defects in the patient's cells were also restored (Fig. 5c and d). Similar results can be observed from the ciliary formation after the WT or mutant CEP295 mRNA transfection (Fig. 5e and f). These results suggest that the P562L variant significantly impairs the function of CEP295, further supporting that the CEP295 variants are the cause of the affected individuals in these two families.

Discussion

CEP295 is required for centriole-to-centrosome conversion and centriole elongation, the depletion of which results in shorter centrioles and reductions in centrosome numbers.[15,25] In addition, pathogenic variants of *RTTN*, which encodes a centrosome-associated protein that functions upstream of CEP295, can lead to primary microcephaly and primordial dwarfism,[26,27] supporting the relevance of CEP295 in the pathogenicity of this phenotype. This study included four individuals with compound heterozygous variants of *CEP295*. They shared common clinical features, including severe microcephaly, short stature, GDD/ID, pachygyria and simplified gyria, and craniofacial and digital abnormalities. Notably, phenotypic analysis of other CEPs showed the features of patients with mutant *CEP295* largely overlapped with those of *CENPJ*- and *CEP152*-associated Seckel syndrome.[28,29] CEP295 can directly interact with CEP152, forming a conserved architectural network essential for centriole-to-centrosome conversion during mitosis in both *Drosophila* and humans.[30] We, therefore, propose terming the phenotype of these four patients as Seckel-like syndrome.

Loss of centrioles in the neural stem cells is thought to be a cause of primary microcephaly, as the spindle positioning is disturbed, leading to a decrease in the pool of neural precursors.[31,32] Defects in centrosomes/centrioles trigger p53-dependent apoptosis, which ultimately contributes to the development of primary microcephaly. In mice, depletion of p53 could rescue cell death and the reduced brain size phenotype.[33] Mechanistically, centrosome loss causes cell arrest at the G_1 phase, which leads to the activation of p53/p21 mediated by USP28 and 53BP1.[16–18] Consistently, after inducing centrosome/centriole defects in the patient-derived fibroblasts, we observed proliferation inhibition and elevated p53/p21 levels in patient's fibroblasts and also in CEP295-depleted U2OS cells. In addition, defects in primary cilia are known to impair various steps of cerebral cortical formation, including progenitor development and neuronal migration, differentiation, and connectivity.[34] Consequently, structural and functional neurological deficits have been widely observed in ciliopathies, such as JBTS and MKS.[35] Similar deficits can also be observed in microcephaly and are associated with some centrosome proteins. For example, CENPJ is essential for cilium disassembly and neurogenesis in the mouse cortex, which is independent of its role in centrosome biogenesis.[36] Here, we showed that CEP295 depletion leads to cilium loss and the formation of shorter cilia in human cells. Additionally, complementary experiments using synthesized CEP295 mRNA showed that the WT CEP295, rather than the P562L mutant, can fully restore the centrosome/centriole and ciliary developmental defects in patient-derived fibroblasts. Though the evidence is limited, we here suggest that the neurodevelopmental delay of the four patients presented in this study may be attributed to the primary microcephaly caused by a combination of defects in centrosome/centriole biogenesis and ciliogenesis.

MKS is a rare autosomal recessive ciliopathy characterized by occipital encephalocele, cystic-dysplastic kidneys, congenital hepatic fibrosis, and polydactyly.[37] Here, we report a stillbirth who was clinically diagnosed with MKS, showing a distinct phenotype from the other four patients. The foetus was presumed to harbour a homozygous deleterious variant of *CEP295* (p. Q868Rfs*25) inherited from his consanguineous parents. As MKS is a lethal ciliopathy,[38] patient 5 did not

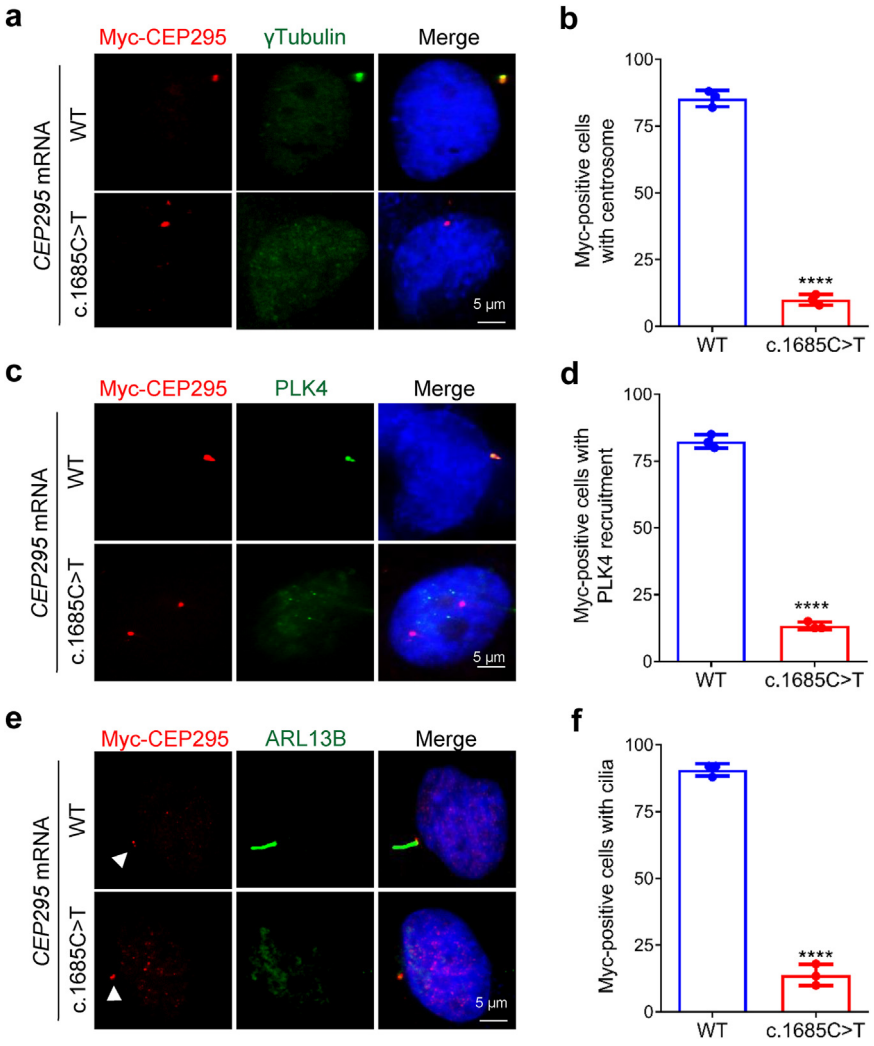

Fig. 5: **The wild-type CEP295, rather than the P562L mutant, can correct the defects of the centrosome and cilia in the patient 1-derived fibroblasts. (a–d)** Immuofluorescence of patient 1's fibroblasts transfected with indicated mRNA, synchronized at S-phase, and stained using antibodies against Myc-tag (red, indicating CEP295) and γ-tubulin (green, indicating centrosome) or PLK4 (green, indicating new mother centriole). Cells with co-localization of Myc and γ-tubulin or PLK4 were quantified **(e, f)** Patient 1's fibroblasts were transfected with indicated mRNA for 48 h, and treated with serum starvation for 24 h before fixation. Cells were processed for immunofluorescence using antibodies against Myc-tag (red, indicating CEP295) and ARL13B (green, indicating cilium). Cells with co-localization of Myc and ARL13B were quantified. n = 3 biologically independent experiments, counting at least 60 cells per experiment. Error bars represent mean ± SD. ****, $P < 0.0001$, two-tailed Student's t-test.

survive, and no biological samples were available to further elucidate ciliary development. Though our findings indicate that *CEP295* variants may be associated with ciliopathy, we cannot exclude the possibility of a *de novo* variant elsewhere in the genome of the foetus. Thus, investigating whether CEP295 deficiency can cause these two distinct phenotypes is necessary in the future. Given that conventional depletion of CEP295 leads to prenatal lethality in mice and zebrafish models (data not shown), constructing conditional knock-in animal models with the point mutations identified from the patients with microcephaly and MKS is the most feasible strategy.

In summary, we have shown bi-allelic loss of functional variants of *CEP295* in patients with primary microcephaly, which we defined as Seckel-like syndrome. This study extends our understanding of the role of CEPs in the pathogenesis of primary microcephaly and Seckel syndrome. Additionally, we demonstrated that the loss of function of CEP295 results in defects in cilium formation and suggested the possible correlation between CEP295 variants and the MKS phenotype.

Contributors

NL, KM and JW conceived the research. NL and JW designed and supervised experiments. YFX, HZC, Guoqiang Li, LNC, GYC and JT conducted experiments for this article. NL, KM and JW acquired and interpretated data and wrote the manuscript; LA, MRB, YG, NB, EF, QHF, XMW and FSA helped in phenotyping the patient; REY, TTY and JW analysed DNA sequencing data. Jingqi Lin and WF designed and implemented mRNA synthesis and transfection. QHF, YPS and FSA helped with manuscript writing and revision. JW, NL, FSA and KM have accessed and verified all data reported in the manuscript, and all authors have read and approved the final version of the manuscript.

Data sharing statement

The WES raw data of patient 1 is available in the Sequence Read Archive public database (https://www.ncbi.nlm.nih.gov/sra) under data series accession number PRJNA719957. Supplementary Material associated with this article can be found in the online version.

Declaration of interests

The authors declare no competing interests.

Acknowledgements

We are deeply grateful to the patients and their families for participating in this study. This study was supported by the National Key Research and Development Program of China (2020YFA0804000, 2022YFC2705200), National Natural Science Foundation of China (82071660, 81900722), the Program of Innovative Research Team of High-Level Local Universities in Shanghai (SHSMU-ZDCX20212200), the Project of Shanghai Municipal Science and Technology Commission (20MC1920400), Shanghai "Rising Stars of Medical Talents" Youth Development Program, and a grant from King Saud University (RSP-2021/181). We also acknowledge the support of King Salman Center for Disability Research through Research Group (RG-2022-010). Authors thank KFMC Research Centre for partial support.

Appendix A. Supplementary data

Supplementary data related to this article can be found at https://doi.org/10.1016/j.ebiom.2023.104940.

References

1 Doxsey S, McCollum D, Theurkauf W. Centrosomes in cellular regulation. *Annu Rev Cell Dev Biol*. 2005;21:411–434.
2 Bettencourt-Dias M, Glover DM. Centrosome biogenesis and function: centrosomics brings new understanding. *Nat Rev Mol Cell Biol*. 2007;8(6):451–463.
3 Prosser SL, Pelletier L. Centriolar satellite biogenesis and function in vertebrate cells. *J Cell Sci*. 2020;133(1).
4 Alves-Cruzeiro JM, Nogales-Cadenas R, Pascual-Montano AD. CentrosomeDB: a new generation of the centrosomal proteins database for Human and Drosophila melanogaster. *Nucleic Acids Res*. 2014;42(Database issue):D430–D436.
5 Kumar A, Rajendran V, Sethumadhavan R, Purohit R. CEP proteins: the knights of centrosome dynasty. *Protoplasma*. 2013;250(5):965–983.
6 Lin YC, Chang CW, Hsu WB, et al. Human microcephaly protein CEP135 binds to hSAS-6 and CPAP, and is required for centriole assembly. *EMBO J*. 2013;32(8):1141–1154.
7 Cizmecioglu O, Arnold M, Bahtz R, et al. Cep152 acts as a scaffold for recruitment of Plk4 and CPAP to the centrosome. *J Cell Biol*. 2010;191(4):731–739.
8 Jayaraman D, Bae BI, Walsh CA. The genetics of primary microcephaly. *Annu Rev Genomics Hum Genet*. 2018;19:177–200.
9 Wang J, Zhang W, Jiang H, Wu BL. Primary Ovarian Insufficiency C. Mutations in HFM1 in recessive primary ovarian insufficiency. *N Engl J Med*. 2014;370(10):972–974.
10 Monies D, Abouelhoda M, Assoum M, et al. Lessons learned from large-scale, first-tier clinical exome sequencing in a highly consanguineous population. *Am J Hum Genet*. 2019;104(6):1182–1201.
11 Ai X, Yan B, Witman N, et al. Transient secretion of VEGF protein from transplanted hiPSC-CMs enhances engraftment and improves rat heart function post MI. *Mol Ther*. 2023;31(1):211–229.
12 Sobreira N, Schiettecatte F, Valle D, Hamosh A. GeneMatcher: a matching tool for connecting investigators with an interest in the same gene. *Hum Mutat*. 2015;36(10):928–930.
13 Tsuchiya Y, Yoshiba S, Gupta A, Watanabe K, Kitagawa D. Cep295 is a conserved scaffold protein required for generation of a bona fide mother centriole. *Nat Commun*. 2016;7:12567.
14 Li H, Ji CY, Zong XN, Zhang YQ. [Body mass index growth curves for Chinese children and adolescents aged 0 to 18 years]. *Zhonghua Er Ke Za Zhi*. 2009;47(7):493–498.
15 Izquierdo D, Wang WJ, Uryu K, Tsou MF. Stabilization of cartwheel-less centrioles for duplication requires CEP295-mediated centriole-to-centrosome conversion. *Cell Rep*. 2014;8(4):957–965.
16 Fong CS, Mazo G, Das T, et al. 53BP1 and USP28 mediate p53-dependent cell cycle arrest in response to centrosome loss and prolonged mitosis. *Elife*. 2016;5.
17 Lambrus BG, Daggubati V, Uetake Y, et al. A USP28-53BP1-p53-p21 signaling axis arrests growth after centrosome loss or prolonged mitosis. *J Cell Biol*. 2016;214(2):143–153.
18 Meitinger F, Anzola JV, Kaulich M, et al. 53BP1 and USP28 mediate p53 activation and G1 arrest after centrosome loss or extended mitotic duration. *J Cell Biol*. 2016;214(2):155–166.
19 Frank V, den Hollander AI, Bruchle NO, et al. Mutations of the CEP290 gene encoding a centrosomal protein cause Meckel-Gruber syndrome. *Hum Mutat*. 2008;29(1):45–52.
20 Akizu N, Silhavy JL, Rosti RO, et al. Mutations in CSPP1 lead to classical Joubert syndrome. *Am J Hum Genet*. 2014;94(1):80–86.
21 Srour M, Hamdan FF, McKnight D, et al. Joubert syndrome in French Canadians and identification of mutations in CEP104. *Am J Hum Genet*. 2015;97(5):744–753.
22 Ho EK, Stearns T. Hedgehog signaling and the primary cilium: implications for spatial and temporal constraints on signaling. *Development*. 2021;148(9).
23 Luo M, Lin Z, Zhu T, et al. Disrupted intraflagellar transport due to IFT74 variants causes Joubert syndrome. *Genet Med*. 2021;23(6):1041–1049.
24 Ai X, Luo R, Wang H, et al. Vascular endothelial growth factor a modified mRNA engineered cellular electrospun membrane complexes promotes mouse skin wound repair. *Mater Today Bio*. 2023;22:100776.
25 Chang CW, Hsu WB, Tsai JJ, Tang CJ, Tang TK. CEP295 interacts with microtubules and is required for centriole elongation. *J Cell Sci*. 2016;129(13):2501–2513.
26 Shamseldin H, Alazami AM, Manning M, et al. RTTN mutations cause primary microcephaly and primordial dwarfism in humans. *Am J Hum Genet*. 2015;97(6):862–868.
27 Kheradmand Kia S, Verbeek E, Engelen E, et al. RTTN mutations link primary cilia function to organization of the human cerebral cortex. *Am J Hum Genet*. 2012;91(3):533–540.
28 Kalay E, Yigit G, Aslan Y, et al. CEP152 is a genome maintenance protein disrupted in Seckel syndrome. *Nat Genet*. 2011;43(1):23–26.
29 Al-Dosari MS, Shaheen R, Colak D, Alkuraya FS. Novel CENPJ mutation causes Seckel syndrome. *J Med Genet*. 2010;47(6):411–414.
30 Fu J, Lipinszki Z, Rangone H, et al. Conserved molecular interactions in centriole-to-centrosome conversion. *Nat Cell Biol*. 2016;18(1):87–99.
31 Basto R, Lau J, Vinogradova T, et al. Flies without centrioles. *Cell*. 2006;125(7):1375–1386.
32 Fish JL, Kosodo Y, Enard W, Paabo S, Huttner WB. Aspm specifically maintains symmetric proliferative divisions of neuroepithelial cells. *Proc Natl Acad Sci U S A*. 2006;103(27):10438–10443.
33 Bazzi H, Anderson KV. Acentriolar mitosis activates a p53-dependent apoptosis pathway in the mouse embryo. *Proc Natl Acad Sci U S A*. 2014;111(15):E1491–E1500.
34 Guemez-Gamboa A, Coufal NG, Gleeson JG. Primary cilia in the developing and mature brain. *Neuron*. 2014;82(3):511–521.
35 Hildebrandt F, Benzing T, Katsanis N. Ciliopathies. *N Engl J Med*. 2011;364(16):1533–1543.
36 Ding W, Wu Q, Sun L, Pan NC, Wang X. Cenpj regulates cilia disassembly and neurogenesis in the developing mouse cortex. *J Neurosci*. 2019;39(11):1994–2010.
37 Barisic I, Boban L, Loane M, et al. Meckel-Gruber Syndrome: a population-based study on prevalence, prenatal diagnosis, clinical features, and survival in Europe. *Eur J Hum Genet*. 2015;23(6):746–752.
38 Hartill V, Szymanska K, Sharif SM, Wheway G, Johnson CA. Meckel-gruber syndrome: an update on diagnosis, clinical management, and research advances. *Front Pediatr*. 2017;5:244.